

Single-Crystal Polarized Optical Absorption Spectroscopy of the One-Dimensional Ferrimagnet $\text{Mn}^{\text{II}}\text{Cu}^{\text{II}}(\text{pba})(\text{H}_2\text{O})_3 \cdot 2\text{H}_2\text{O}$ (pba = 1,3-Propylenebis(oxamato))

Olivier Cador, Corine Mathonière,* and Olivier Kahn

Laboratoire des Sciences Moléculaires, Institut de Chimie de la Matière Condensée de Bordeaux, UPR CNRS No. 9048, 33608 Pessac, France

Received October 26, 1999

Powder and single-crystal optical absorption of the ferrimagnet $\text{Mn}^{\text{II}}\text{Cu}^{\text{II}}(\text{pba})(\text{H}_2\text{O})_3 \cdot 2\text{H}_2\text{O}$ (denoted MnCu) and the Mn-doped compound $\text{Mn}_{0.1}\text{Mg}_{0.9}\text{Cu}(\text{pba})(\text{H}_2\text{O})_3 \cdot 2\text{H}_2\text{O}$ (denoted $\text{Mn}_{0.1}\text{Mg}_{0.9}\text{Cu}$) with pba standing for 1,3-propylenebis(oxamato) was investigated in the 10–300 K range. The crystal structure of MnCu was previously reported, and consists of bimetallic chains with octahedral Mn^{II} and square pyramidal Cu^{II} ions linked by oxamato bridges, MnCu and $\text{Mn}_{0.1}\text{Mg}_{0.9}\text{Cu}$ being isostructural. The spectra of both MnCu and $\text{Mn}_{0.1}\text{Mg}_{0.9}\text{Cu}$ show an important dichroism along the chain direction, due to the strong polarization of the Cu^{II} band at around 16 000 cm^{-1} in this direction. They exhibit narrow and intense spin-forbidden Mn^{II} transitions in the 24000–25000 cm^{-1} range, which are activated by an exchange mechanism. The polarization and thermal dependence of the ${}^6\text{A}_{1\text{g}} \rightarrow {}^4\text{A}_{1\text{g}}, {}^4\text{E}_{\text{g}}(\text{G})$ Mn^{II} transitions were recorded. The polarization along the chain axis was interpreted in the framework of the pair mechanism first introduced by Tanabe and co-workers. A theoretical expression for the thermal dependence of the intensity was derived by considering the Cu^{II} spin as a quantum spin and the Mn^{II} spin as a classical spin, and compared with the experimental data. The interaction parameter between the local ground states has been found to be $J = -25 \text{ cm}^{-1}$ using the spin Hamiltonian $\mathbf{H} = -J\sum_i(\mathbf{S}_{\text{Mn},i}\mathbf{S}_{\text{Cu},i} + \mathbf{S}_{\text{Mn},i+1}\mathbf{S}_{\text{Cu},i})$. The spectra of $\text{Mn}_{0.1}\text{Mg}_{0.9}\text{Cu}$ showed cold and hot bands, whose energy difference is directly related to J and the interaction parameter J^* between the Cu^{II} ion in its ground state and the Mn^{II} ion in its spin-flip excited state. J^* has been estimated to be $+40 \text{ cm}^{-1}$. These results have been compared to those obtained with other $\text{Mn}^{\text{II}}\text{Cu}^{\text{II}}$ compounds. The complementarity between optical and magnetic properties has been discussed.

Introduction

The field of molecular magnetism has been a very active area of research for more than two decades. One of the challenges in this field is the design of molecule-based magnets from paramagnetic molecular bricks. By using the synthetic procedures of molecular/coordination chemistry, the preparation of a room-temperature molecule-based magnet¹ or of very hard magnets^{2,3} with coercive fields of several teslas is no more a dream. Furthermore, these materials are often weakly colored, and the synergy of optical and magnetic properties might lead to potential applications in the field of magneto-optical devices. Recently, photomagnetic effects in Prussian blue-like compounds were reported where light irradiation was used to raise the critical temperature of a magnet,⁴ or to reverse the magnetization direction.⁵

Until now, spectroscopic studies of exchange-coupled systems mainly involved doped systems, which are homometallic or bimetallic. However, the information deduced from the optical studies could not be easily correlated to that deduced from

magnetic studies. A few years ago, we initiated a project concerning the absorption spectroscopy of exchange-coupled bimetallic $\text{Mn}^{\text{II}}\text{Cu}^{\text{II}}$ systems. Several molecular topologies have been studied with oxamato or oxamido bridges between the metal ions. The exchange interaction between Mn^{II} and Cu^{II} ions gave rise to a huge enhancement of the intensity of the formally spin-forbidden Mn^{II} transitions. The exchange-induced absorption mechanism, first proposed by Tanabe and co-workers during the 1960s,⁶ was successfully used to interpret the thermal behavior of ${}^6\text{A}_{1\text{g}} \rightarrow {}^4\text{A}_{1\text{g}}, {}^4\text{E}_{\text{g}}(\text{G})$ Mn^{II} transitions. The interaction parameter when the metal ions are in their electronic ground state was determined from spectroscopic data and found to be in agreement with the value deduced from magnetic measurements.^{7–10} We also succeeded in estimating the value of the interaction parameter J^* between Cu^{II} in its ground state and one Mn^{II} in its spin-flip excited state,^{8–10} which otherwise cannot be deduced from magnetic measurements. For a linear triad, $\text{Cu}^{\text{II}}\text{Mn}^{\text{II}}\text{Cu}^{\text{II}}$, it was surprising that the interaction is antiferromagnetic (J negative) in the ground state, and ferromagnetic (J positive) in the spin-flip excited state.¹⁰

So far, the structure of the compounds investigated consisted of isolated molecules that modeled the repeating units in

- (1) Ferlay, S.; Mallah, T.; Ouahes, R.; Veillet, P.; Verdager, M. *Nature* **1995**, *70*, 701.
- (2) Kurmoo, M.; Keppert, C. J. *New J. Chem.* **1998**, *22*, 1515.
- (3) Vaz, M. G. F.; Pinheiro, L. M. M.; Stumpf, H. O.; Alcantara, A. F. C.; Golhen, S.; Ouahab, L.; Cador, O.; Mathonière, C.; Kahn, O. *Chem. Eur.* **1999**, *5*, 1486.
- (4) (a) Sato, O.; Iyoda, T.; Fujishima, K.; Hashimoto, K. *Science* **1996**, *272*, 704. (b) Sato, O.; Einaga, Y.; Fujishima, A.; Hashimoto, K. *Inorg. Chem.* **1999**, *38*, 4405.
- (5) (a) Ohkoshi, S.; Yorozu, S.; Sato, O.; Fujishima, A. *Appl. Phys. Lett.* **1997**, *70*, 1040. (b) Ohkoshi, S.; Hashimoto, K. *J. Am. Chem. Soc.* **1999**, *121*, 10591.

- (6) (a) Ferguson, J.; Guggenheim, H. J.; Tanabe, Y. *J. Phys. Soc. Jpn.* **1966**, *21*, 692. (b) Ferguson, J.; Guggenheim, H. J.; Tanabe, Y. *J. Chem. Phys.* **1966**, *45*, 1134.
- (7) Mathonière, C.; Kahn, O.; Daran, J. C.; Hilbig, H.; Köhler, F. H. *Inorg. Chem.* **1993**, *32*, 4057.
- (8) Mathonière, C.; Kahn, O. *Inorg. Chem.* **1994**, *33*, 2103.
- (9) Cador, O.; Mathonière, C.; Kahn, O. *Inorg. Chem.* **1997**, *36*, 1923.
- (10) Cador, O.; Mathonière, C.; Kahn, O.; Costes, J. P.; Verelst, M.; Lecante, P. *Inorg. Chem.* **1999**, *38*, 2643.

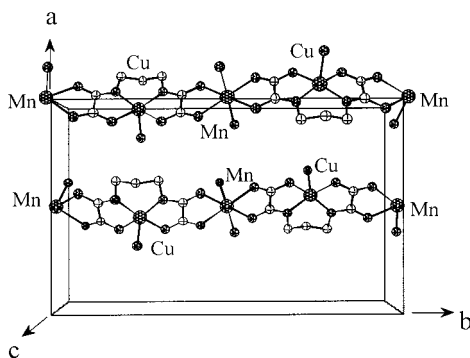


Figure 1. Structure of the compound MnCu. The noncoordinated water molecules were omitted for clarity.

polymeric one- or two-dimensional systems exhibiting long-range magnetic ordering.^{11,12} The theoretical determination of the thermal dependence of the ${}^6A_{1g} \rightarrow {}^4A_{1g}$, ${}^4E_g(G)$ Mn^{II} transitions implicated the calculation of matrix elements of the transition moment between discrete energy levels. Investigations were performed in solution or with powder samples when no single crystals large enough for spectroscopic measurements could be obtained. This paper is devoted to the single-crystal and powder absorption spectroscopy of the chain compound with the formula MnCu(pba)(H₂O)₃·2H₂O abbreviated as MnCu, where pba = 1,3-propylenebis(oxamato). The compound crystallizes in the space group *Pnma*, *Z* = 4, and does not exhibit significant structural change between room temperature and 10 K.¹³ It consists of ordered bimetallic chains with octahedral Mn^{II} and square pyramidal Cu^{II} ions bridged by oxamato groups (Figure 1). The Mn^{II} ion situated at a center of symmetry completes its coordination sphere with two water molecules in trans configuration while the Cu^{II} ions are located on a crystallographic mirror plane. The chains run along the crystallographic *b* axis, and are linked together through a hydrogen-bonding network.

The spectroscopic data will be interpreted using a formalism developed by Tanabe. The one-dimensional character of the compound leads to a spectrum of continuous energy levels which excludes the use of simple techniques and hence requires a rather elaborate theoretical treatment. Results from MnCu will be compared to those from the Mn-doped MgCu(pba)(H₂O)₃·2H₂O compound abbreviated as Mn_{0.1}Mg_{0.9}Cu (molar ratio Mg/Mn = 9).

Experimental Section

MnCu was obtained as a microcrystalline powder or well-shaped light blue single crystals according to reported procedures.^{13a} The doped compound Mn_{0.1}Mg_{0.9}Cu, synthesized using a mixture of magnesium(II) and manganese(II) chlorides, was obtained as well-shaped blue single crystals. The extent of Mn doping was determined by atomic absorption spectroscopy. Single-crystal X-ray diffraction confirmed that MnCu and Mn_{0.1}Mg_{0.9}Cu are isostructural.

The orientation of the crystallographic axes with respect to the morphology of the crystal was determined by X-ray diffraction. In both compounds, the extinction directions coincide with the crystallographic axes. The optical absorption spectra were recorded on a CARY 5E spectrophotometer equipped with a continuous-flow helium cryostat

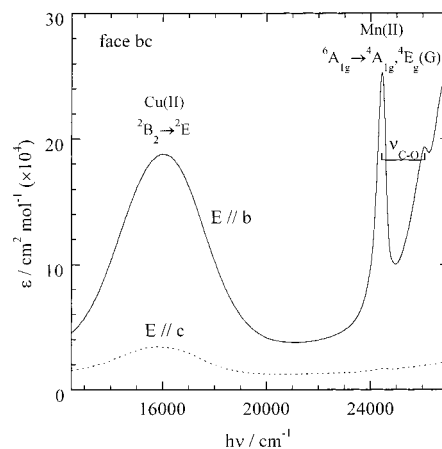


Figure 2. Polarized optical absorption spectra at room temperature perpendicularly to the *bc* face of a single crystal of MnCu: *E*//*b* (solid line) and *E*//*c* (dashed line).

(Oxford Instruments) operating in the temperature range of 4–300 K. Powder samples of MnCu were studied as pellets prepared as follows: the microcrystalline powder was compacted with a cylinder press (2 tons of pressure for 90 min), then stuck on a glass plate with cyanolite, and polished to make it sufficiently transparent. Glan–Taylor prisms were used to record the polarized absorption spectra with the electric field *E* parallel to the three crystallographic axes. Baseline correction was applied to the spectra in the 24000–25200 cm⁻¹ range by connecting the unique tangent between two points situated on either side of the absorption band. Band intensities were calculated from the area covered by the spectrum and the linear baseline. The magnetic susceptibility of MnCu was measured on a Quantum Design MPMS-5S SQUID magnetometer in the 2–300 K temperature range with a dc magnetic field of 1 kOe.

Results

The magnetic behavior of MnCu was previously described in ref 13a. This compound may be considered as an archetype of a one-dimensional ferrimagnet. The $\chi_M T$ versus *T* plot (χ_M being the molar magnetic susceptibility per formula unit and *T* the temperature) presents a characteristic minimum at around 100 K, and increases rapidly as *T* is lowered further below this temperature. The compound MnCu exhibits an antiferromagnetic long-range ordering at 2.2 K, and its pellet form behaves in the same fashion. This behavior is characteristic of a Mn^{II}Cu^{II} alternating chain with strong intrachain antiferromagnetic interaction on which very weak interchain interactions are superimposed. The value of the intrachain interaction parameter *J* was determined from these magnetic susceptibility data using a model where *S*_{Mn} is treated as a classical spin and *s*_{Cu} as a quantum spin.¹⁴ Using the spin Hamiltonian $\mathbf{H} = -J\sum_i(\mathbf{S}_{Mn,i}\mathbf{s}_{Cu,i} + \mathbf{S}_{Mn,i+1}\mathbf{s}_{Cu,i})$ in the temperature range of 40–300 K yielded a *J* value of -25 cm⁻¹.

The room-temperature polarized absorption spectrum of MnCu with light polarized along the crystallographic *b* and *c* axes (*E*//*b* and *E*//*c*) is represented in Figure 2. The *E*//*a* spectra are similar to the *E*//*c* spectra at room temperature, and can be divided into two regions: (i) the copper region corresponding to the broad band centered at 16 000 cm⁻¹ for both *E*//*b* and *E*//*c* and strongly polarized in the *b* direction; (ii) the manganese region in the higher energy range which constitutes two narrow bands centered at 24 400 and 26 050 cm⁻¹ which are almost fully polarized in the *b* direction. The manganese bands are superimposed on the low-energy side of a very intense band centered in the far UV which appears to be fully polarized in

(11) Pei, Y.; Verdaguer, M.; Kahn, O.; Sletten, J.; Renard, J. P. *J. Am. Chem. Soc.* **1986**, *108*, 7428.

(12) Stumpf, H. O.; Pei, Y.; Kahn, O.; Sletten, J.; Renard, J. P. *J. Am. Chem. Soc.* **1993**, *115*, 6738.

(13) (a) Pei, Y.; Verdaguer, M.; Kahn, O.; Sletten, J.; Renard, J. P. *Inorg. Chem.* **1987**, *26*, 138. (b) Baron, V.; Gillon, B.; Cousson, A.; Mathonière, C.; Kahn, O.; Grand, A.; Ohrström, L.; Delley, B.; Bonnet, M.; Boucherle, J. X. *J. Am. Chem. Soc.* **1997**, *119*, 3500.

(14) Seiden, J. *J. Phys. Lett.* **1983**, *44*, L947.

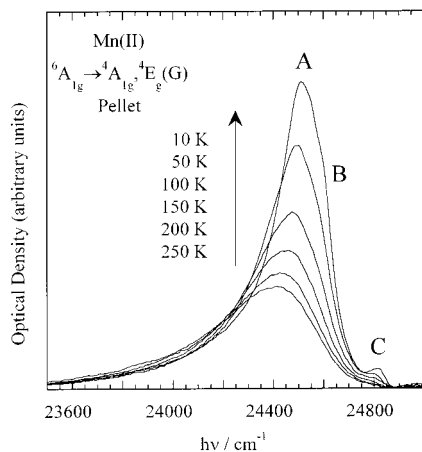


Figure 3. Baseline-corrected powder spectra of MnCu in the 23500–25100 cm^{-1} range at various temperatures.

the *b* direction. The intensity and polarization along the chain axis of this very intense band can be attributed to $\text{Cu}^{\text{II}} \rightarrow \text{oxamato}$ or $\text{Cu}^{\text{II}} \rightarrow \text{Mn}^{\text{II}}$ electron transfer. The broad band at 16 000 cm^{-1} is attributed to the ${}^2\text{B}_2 \rightarrow {}^2\text{E}$ d–d electronic transition of Cu^{II} in the idealized C_{4v} symmetry. The color of the single crystals is dark blue along $\mathbf{E} // b$ and light blue along $\mathbf{E} // c$. This dichroism is clearly due to the polarization of the copper band whose origin will be discussed below. The narrow band at 24 450 cm^{-1} is attributed to the ${}^6\text{A}_{1g} \rightarrow {}^4\text{A}_{1g}, {}^4\text{E}_g(\text{G})$ d–d transitions of Mn^{II} in the idealized C_{4v} symmetry. These transitions correspond to pure spin-flips and are not influenced by the ligand field at the first order. The origin of the band at 26 070 cm^{-1} is uncertain, but it is tentatively assigned to the quantum of the vibration $\nu_{\text{C-O}}$ ($\sim 1625 \text{ cm}^{-1}$) of the oxamato group, built on the ${}^6\text{A}_{1g} \rightarrow {}^4\text{A}_{1g}, {}^4\text{E}_g(\text{G})$ electronic transitions.

In contrast to the copper band, the band associated with the electronic transitions ${}^6\text{A}_{1g} \rightarrow {}^4\text{A}_{1g}, {}^4\text{E}_g(\text{G})$ displays a great enhancement of its intensity as the temperature is lowered. Saturation effects are observed at low temperature when single crystals are worked with; hence, we decided to work with pellets. Since the intensity of $\mathbf{E} // a$ and $\mathbf{E} // c$ is extremely weak with respect to $\mathbf{E} // b$, it may be considered that the pellet spectrum corresponds to that for light polarized along the *b* direction. Figure 3 shows the temperature dependence of the ${}^6\text{A}_{1g} \rightarrow {}^4\text{A}_{1g}, {}^4\text{E}_g(\text{G})$ Mn^{II} transitions. The spectrum mainly constitutes of one band, denoted A, with a maximum at 24 515 cm^{-1} at 10 K and 24 415 cm^{-1} at 250 K. The intensity of band A increases as the temperature is lowered; hence, it is a cold band. At low temperature, new features appear, namely, a shoulder denoted B and a new band denoted C, approximately centered at 24 600 and 24 815 cm^{-1} , respectively, at 10 K. Since transition to the ${}^4\text{A}_1$ state has always been found to be more intense than the transition to the ${}^4\text{E}$ state, band A is assigned to ${}^6\text{A}_1 \rightarrow {}^4\text{A}_1$ and band B to ${}^6\text{A}_1 \rightarrow {}^4\text{E}$. The origin of band C is unclear since the intensity ratio between bands C and A is not constant from one experiment to the other.

We have already mentioned that the $\mathbf{E} // a$ and $\mathbf{E} // c$ absorption spectra are similar at room temperature, but this is no longer true at lower temperature. The spectra were recorded using a thicker single crystal to increase the absolute intensity of the manganese absorption bands in the $\mathbf{E} // a$ and $\mathbf{E} // c$ directions. The temperature dependence of the $\mathbf{E} // a$ and $\mathbf{E} // c$ absorption spectra in the ${}^6\text{A}_{1g} \rightarrow {}^4\text{A}_{1g}, {}^4\text{E}_g(\text{G})$ region is represented in Figure 4. Three bands are evident in the $\mathbf{E} // a$ spectrum at 10 K; the most intense peak is located almost at the same energy (24 540 cm^{-1}) as band A when observed on a pellet at 10 K and has

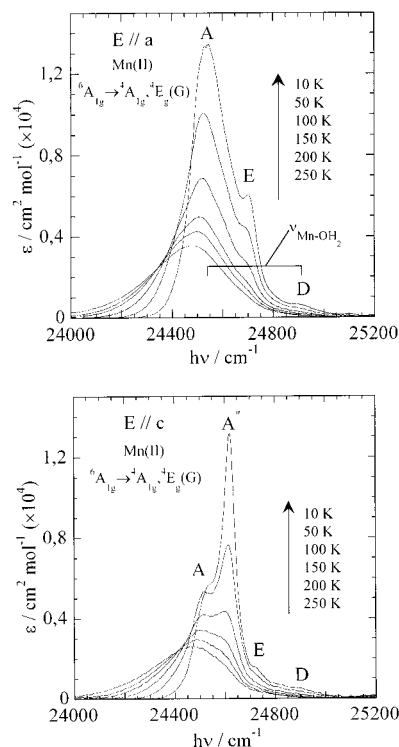


Figure 4. Baseline-corrected polarized spectra of MnCu in the 24000–25200 cm^{-1} range: $\mathbf{E} // a$ (top) and $\mathbf{E} // c$ (bottom) at various temperatures.

similar thermal behavior. The peak is assigned to the ${}^6\text{A}_1 \rightarrow {}^4\text{A}_1$ Mn^{II} transition. The other two, denoted E and D, are centered at 24 710 and 24 915 cm^{-1} , respectively, at 10 K. Their intensities also increase as the temperature decreases. In addition to the three bands A, E, and D, the $\mathbf{E} // c$ spectrum contains an additional narrow band denoted A'' centered at 24 620 cm^{-1} , nearly at the same energy as band B (24 600 cm^{-1}) observed on the pellet spectrum (Figure 3). Band A'' is the most intense at 10 K, while its intensity is negligible with respect to band A at 250 K. We later discuss the possible origins of band A''. Although it is not possible to deconvolute the spectra, bands A in the $\mathbf{E} // c$ and $\mathbf{E} // a$ spectra have significantly different thermal behaviors. The increase in intensity as the temperature is lowered is less pronounced for the $\mathbf{E} // c$ spectrum. The energy of band D is 375 cm^{-1} higher than that of band A, which is close to the energy of the stretching vibration $\nu_{\text{Mn-O}(\text{water})}$. Therefore, band D can be assigned to a vibronic transition built on the electronic transition ${}^6\text{A}_1 \rightarrow {}^4\text{A}_1$. In the low-energy region of the spectra ($\sim 24\,300 \text{ cm}^{-1}$), the absorption coefficients, for both $\mathbf{E} // a$ and $\mathbf{E} // c$, increase significantly as the system is warmed, suggesting the presence of hot bands. This effect is very weak in Figure 3 and may be due to the increase of the bandwidth with pellets compared to single crystals.

Further, in our investigation, we studied the doped compound $\text{Mn}_{0.1}\text{Mg}_{0.9}\text{Cu}$. Single crystals of this compound display the same dichroism as the pure MnCu. The $\mathbf{E} // b$ spectrum between 10 and 250 K is represented in Figure 5. The $\mathbf{E} // a$ and $\mathbf{E} // c$ spectra recorded at $T = 20 \text{ K}$ in the region of the ${}^6\text{A}_{1g} \rightarrow {}^4\text{A}_{1g}, {}^4\text{E}_g(\text{G})$ Mn^{II} transitions are shown in Figure 6. In the $\mathbf{E} // b$ spectrum, four bands are observed, denoted A_1' , A_1 , A_1'' , and B_1 , which are centered at 24 325, 24 480, 24 540, and 24 625 cm^{-1} , respectively. These spectra are similar to those obtained for the trinuclear molecular compound $\text{Mn}[\text{CuL}]_2 \cdot 5\text{H}_2\text{O}$,¹⁰ which are composed of three bands of types A_1' , A_1 , and B_1 located at the same positions and with the same thermal behavior. A_1' is a hot band, while A_1 and B_1 are cold bands. The $\mathbf{E} // a$ and

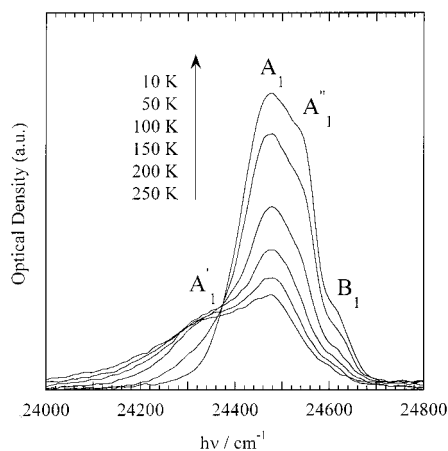


Figure 5. Baseline-corrected polarized spectra $E//b$ of $Mn_{0.1}Mg_{0.9}Cu$ in the 24000–24800 cm^{-1} range at various temperatures.

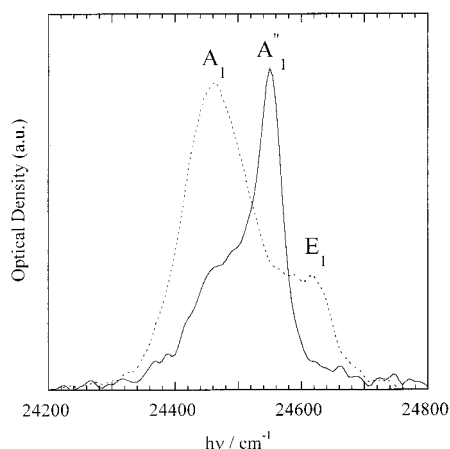


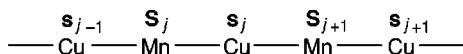
Figure 6. Baseline-corrected polarized spectra of $Mn_{0.1}Mg_{0.9}Cu$ in the 24200–24800 cm^{-1} range: $E//c$ (solid line) and $E//a$ (dashed line) at 20 K.

$E//c$ spectra recorded at $T = 20$ K have the same spectral characteristics as $MnCu$ (see above) with a red shift of about 80 cm^{-1} . It is important to note that the intensity ratio between the bands found in the $E//a$ and $E//c$ spectra and their thermal behaviors are identical to those measured for $MnCu$.

Quantitative Interpretation

In 1971, Shinagawa and co-workers derived an analytical expression for the thermal dependence of the intensity of spin-forbidden transitions activated by an exchange mechanism in a two-sublattice antiferromagnet.¹⁵ This model was later extended to a one-dimensional antiferromagnet by Ebara and co-workers.¹⁶ Our objective is to adapt this model to the one-dimensional ferrimagnet $MnCu$ to quantitatively interpret the temperature dependence of the ${}^6A_{1g} \rightarrow {}^4A_{1g}, {}^4E_g(G)$ Mn^{II} transitions.

For $MnCu$, the coupling scheme within the chain is shown below:



Only the nearest neighbors of the Mn^{II} ions are considered, so that the intensity absorbed by the j th Mn^{II} ion in one chain for a light polarization direction ξ is given by

$$I_j^\xi(T) = \sum_{k,k'=j-1} \langle P_{j,k}^\dagger P_{j,k'}^\xi \rangle \quad \text{with} \quad \mathbf{P}_{j,k} = \sum_{i=1}^5 \pi_{Mn_i, jCu_k} (\mathbf{s}_{Mn_i, j} \cdot \mathbf{s}_{Cu_k}) \quad (1)$$

where the angular brackets mean thermal average and the symbol \dagger stands for *adjoint* operator. $\mathbf{P}_{j,k}$ is the spin-dependent dipolar moment, first introduced by Tanabe,^{6a} $\mathbf{s}_{Mn_i, j}$ is the mono-electronic spin operator which refers to the i th 3d orbital of the j th Mn^{II} ion, \mathbf{s}_{Cu_k} is the spin operator referring to the singly occupied orbital of the k th Cu^{II} ion, and π_{Mn_i, jCu_k} is a component of the exchange-induced dipolar moment defined as

$$\pi_{Mn_i, jCu_k}^\xi = (\partial J_{i,j,k} / \partial E_{E\xi}^\xi)_{E\xi \rightarrow 0} \quad (2)$$

where $J_{i,j,k}$ is the interaction parameter between the i th 3d orbital of the j th Mn^{II} ion and the magnetic orbital of the k th Cu^{II} ion. The excited states ${}^4A_{1g}$ and ${}^4E_g(G)$ do not contain orbital contributions, and the π_{Mn_i, jCu_k} coefficients can be considered as vectors. Following the procedure given in ref 15, the intensity can be written in terms of ground-state spin operators, as follows:

$$I_j^\xi(T) = \sum_{k,k'=j-1} \Pi_{j,k}^\xi \Pi_{j,k'}^\xi \left[\frac{1}{6} \langle \mathbf{s}_k \cdot \mathbf{s}_{k'} \rangle + \frac{i}{4S_j} \langle \mathbf{S}_j \cdot [\mathbf{s}_k \times \mathbf{s}_{k'}] \rangle - \frac{1}{2S_j(2S_j - 1)} \langle \mathbf{s}_k \cdot \mathbf{Q}_j \cdot \mathbf{s}_{k'} \rangle \right] \quad (3)$$

with

$$Q_{j\alpha\beta} = \frac{1}{2} (S_{j\alpha} S_{j\beta} + S_{j\beta} S_{j\alpha}) - \frac{1}{3} \delta_{\alpha\beta} S_j (S_j + 1) \quad \alpha, \beta = x, y, z \quad (4)$$

and

$$\Pi_{j,k}^\xi = \sum_{i=1}^5 \pi_{Mn_i, jCu_k}^\xi \left(\frac{2}{2S_j + 1} \right)^{1/2} \langle {}^6A_{1g} | \mathbf{s}_{Mn_i, j} | {}^4A_{1g}, {}^4E_g \rangle \quad (5)$$

Equation 3 is obtained without any approximation and does not require the explicit description of the excited state, except through the reduced matrix elements appearing in the definition of $\Pi_{j,k}$ coefficients in eq 5.

Assuming a symmetry of C_{2v} for each Mn_jCu_k pair with the 2-fold axis collinear to the chain axis, the vectors π_{Mn_i, jCu_k} are collinear to the b axis.⁹ As the Mn^{II} ions are located on an inversion center, then it follows that

$$\Pi_{j,j-1} = -\Pi_{j,j} = -\Pi_{j,j} \mathbf{b} \quad (6)$$

The problem is now reduced to the calculation of spin correlation functions in eq 3. This can be done with the operator \mathbf{S}_{Mn} treated as a classical spin, i.e., a vector of length $[S_{Mn}(S_{Mn} + 1)]^{1/2}$, and \mathbf{s}_{Cu} as a quantum spin. Some of the spin correlation functions appearing in eq 3 have already been determined by Seiden.¹⁴ The complete set of the correlation functions with the calculation details are given as Supporting Information. The final expression for the intensity is

$$I_j(T) = 2(\Pi_{j,j}^b)^2 \left[\frac{1}{6} s_{Cu} (s_{Cu} + 1) + \frac{1}{4S_{Mn}} \Lambda s_{Cu} [S_{Mn}(S_{Mn} + 1)]^{1/2} - \frac{1}{6} \Lambda^2 s_{Cu}^2 + \frac{S_{Mn} + 1}{3(2S_{Mn} - 1)} \Lambda^2 s_{Cu}^2 \right] \quad (7)$$

with $S_{Mn} = 5/2$ and $s_{Cu} = 1/2$. The expression of the Λ function is given in the Appendix.

(15) Shinagawa, K.; Tanabe, Y. *J. Phys. Soc. Jpn.* **1971**, *30*, 1280.

(16) Ebara, K.; Tanabe, Y. *J. Phys. Soc. Jpn.* **1974**, *36*, 93.

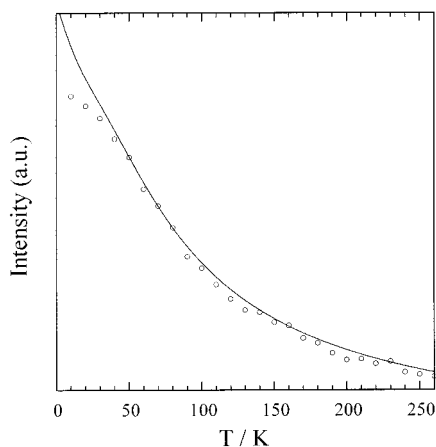


Figure 7. Temperature dependence of the ${}^6\text{A}_{1g} \rightarrow {}^4\text{A}_{1g}$, ${}^4\text{E}_g(\text{G})$ Mn^{II} transitions for MnCu : experimental data (circles) and calculated curve (solid line).

Defining $A = \sum_{i=1}^5 \tau_{\text{Mn}^{\text{II}}\text{Cu}^{\text{II}}}^b \langle {}^6\text{A}_{1g} | \mathbf{S}_{\text{Mn}^{\text{II}}} | {}^4\text{A}_{1g}, {}^4\text{E}_g \rangle$, the high-temperature limit $I_f(\infty)$ is given by

$$I_f(\infty) = A^2/12 \quad (8)$$

which exactly corresponds to twice the high-temperature limit for a pair $\text{Mn}^{\text{II}}\text{Cu}^{\text{II}}$.

Equation 7 was used to fit the pellet spectrum data with $\prod_{j,j}^b$ as constants. The best agreement between experimental and calculated temperature dependencies of the intensity (shown in Figure 7) was obtained with $J = -25 \text{ cm}^{-1}$. This agreement is nearly perfect for $T > 40 \text{ K}$. But a discrepancy was observed for $T < 30 \text{ K}$. This may have two origins: first, the classical spin approximation for \mathbf{S}_{Mn} may not be valid at low temperature due to the quantum fluctuation effects and, second, the interchain interactions, neglected in our model, could play a role at low temperature.

Discussion

The motivations of this optical investigation were 2-fold. First, single crystals were available, so that experiments on polarization effects predicted by the exchange-induced absorption mechanism could be performed. Second, the polymeric nature of MnCu allowed us to treat for the first time the problem of dimensionality. In this section, we further discuss these two aspects.

The important dichroism displayed by the compounds is due to the strong polarization of the Cu^{II} band around $16\,000 \text{ cm}^{-1}$ along the b direction. In the idealized C_{4v} symmetry for the CuN_2O_3 core, the ${}^2\text{B}_2 \rightarrow {}^2\text{E}$ Cu^{II} transition is polarized within the plane defined by two nitrogen and two oxygen atoms coming from two oxamato groups. The structural data show that these planes form two groups, making an angle of 90° between them (Figure 8). The ratio between the intensities in the c and b directions should be 1:2, while the experimental ratio is around 1:5. This difference could be due to the vibronic coupling between charge-transfer states ($\text{Cu}^{\text{II}} \rightarrow \text{oxamato}$ and/or $\text{Cu}^{\text{II}} \rightarrow \text{Mn}^{\text{II}}$ in the UV range) and d-d transitions of Cu^{II} , which increases the intensity along the b direction. The pair mechanism proposed by Tanabe predicts that the ${}^6\text{A}_{1g} \rightarrow {}^4\text{A}_{1g}$, ${}^4\text{E}_g(\text{G})$ Mn^{II} transitions are polarized along the chain direction, which corresponds to the b crystallographic axis. The theory is very well confirmed by experimental results.

Going back to the features of Mn^{II} transitions in $\mathbf{E} // c$ and $\mathbf{E} // a$ spectra, the intensity of the absorption bands increases as

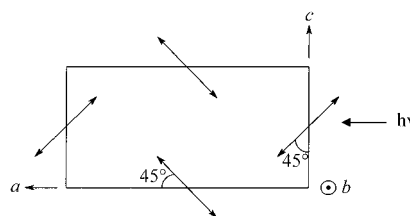


Figure 8. Schematic representation of the chain packing in the ac face of a MnCu crystal. Arrows represent the ac face projection of the planes defined by the two oxygen atoms and two nitrogen atoms surrounding Cu^{II} ions.

the temperature is lowered for both polarization directions. A single ion mechanism can be ruled out since these bands probably have their origin from the exchange mechanism. However, this mechanism should lead to b polarization only, but in fact, the oxamato ligand creates a symmetry slightly lower than C_{2v} for the $\text{Mn}^{2+}\text{Cu}^{2+}$ unit. The exchange mechanism consequently gives a small contribution to the intensity perpendicularly to the chain axis. Furthermore, the Mn and Cu sites are not perfectly aligned within the chains; i.e., the axes joining two adjacent Mn and Cu sites make an angle of $\pm 11^\circ$ with the b axis, which provides some intensity along the a and c directions. The Mn ion being on an inversion center, it is finally straightforward to demonstrate that the resulting intensities in these two directions have the same expression as that given in eq 7. The comparison between experimental and theoretical curves leads to the following J values: -22.6 cm^{-1} for the a direction and -26 cm^{-1} for the c direction. These results confirm that the observed phenomena in the a and c directions arise from an exchange mechanism. According to the well-documented Mn^{2+} spectroscopy,¹⁷ the band assignments should be simple, but the origin of band A'' , which is strongly polarized in the c direction, remains unclear. However, the a and c directions should be equivalent as far as the Mn sites are concerned, and no differences are expected between the $\mathbf{E} // a$ and $\mathbf{E} // c$ spectra in the region of the ${}^6\text{A}_{1g} \rightarrow {}^4\text{A}_{1g}$, ${}^4\text{E}_g(\text{G})$ Mn^{II} transitions. Band A'' in MnCu appears as A_1'' in $\text{Mn}_{0.1}\text{Mg}_{0.9}\text{Cu}$, which is essentially composed of isolated $\text{Cu}^{\text{II}}\text{Mn}^{\text{II}}\text{Cu}^{\text{II}}$ triads. Therefore, this cannot be due to a magnetic ordering effect, although we did not investigate the optical properties in the antiferromagnetically ordered phase below 2.2 K .

In this paper, the Tanabe formalism has been extended to the chain topology. The J value is identical to that deduced from the magnetic data using the same classical approximation for the Mn^{II} spin. This formalism, used to successfully interpret the thermal behavior of formally spin-forbidden Mn^{II} transitions in bimetallic $\text{Mn}^{\text{II}}\text{Cu}^{\text{II}}$ isolated molecules, remains valid for a $\text{Mn}^{\text{II}}\text{Cu}^{\text{II}}$ chain. Nevertheless, in contrast with what had been done for the zero-dimensional compounds,⁸⁻¹⁰ the one-dimensional nature of the compound MnCu did not allow us to determine the interaction parameter J^* in the excited state. The doping technique is not widely used in molecular chemistry; however, it proved to be very helpful in our case. Doping a $\text{Mg}^{\text{II}}\text{Cu}^{\text{II}}$ chain with a small amount of Mn^{II} ions results in the formation of linear triads $\text{Cu}^{\text{II}}\text{Mn}^{\text{II}}\text{Cu}^{\text{II}}$, where the energy difference between the cold band A_1 and the hot band A_1' is directly related to the interaction parameters J and J^* .¹⁰ Assuming that J has the same value of -25 cm^{-1} for MnCu and $\text{Mn}_{0.1}\text{Mg}_{0.9}\text{Cu}$ results in $J^* = +40 \text{ cm}^{-1}$. This positive J^* value means that the interaction is ferromagnetic in the excited state while it is antiferromagnetic in the ground state. This

(17) MacCarthy, P. J.; Güdel, H. U. *Coord. Chem.* **1988**, *88*, 69 and references therein.

surprising result has already been obtained from a linear oxamato-bridged trinuclear compound, $\text{Cu}^{\text{II}}\text{Mn}^{\text{II}}\text{Cu}^{\text{II}}$, which we recently studied.¹⁰ Antiferromagnetic interaction in the ground state and ferromagnetic interaction in the excited state were also reported by Ferré¹⁸ and Ferguson¹⁹ in other compounds. Theoretical calculations are in progress to understand the reasons for this change of sign.

Conclusion

To the best of our knowledge, this work represents the first study of optical absorption spectroscopy for a one-dimensional ferrimagnetic compound. The temperature dependence of the intensity of Mn^{II} spin-forbidden transitions was interpreted quantitatively. Excellent agreement was obtained between the J values deduced from optical and magnetic investigations. Up to now, quantitative analysis of the temperature dependence of spin-forbidden transitions in extended systems based on the Tanabe formalism has been performed in manganese chain compounds.^{16,20} This formalism is also well adapted to the case of extended bimetallic $\text{Mn}^{\text{II}}\text{Cu}^{\text{II}}$ chains and should be used for investigations of more sophisticated $\text{Mn}^{\text{II}}\text{Cu}^{\text{II}}$ systems.

Another novel aspect of this work concerns the polarized optical measurements for both pure heteropolymetallic and doped systems. The polarization of the ${}^6\text{A}_{1g} \rightarrow {}^4\text{A}_{1g}$, ${}^4\text{E}_g(\text{G})$ Mn^{II} transitions along the b axis (the chain axis) confirms that the exchange mechanism is very efficient for these spin-flip transitions. Single-crystal spectroscopy also reveals exchange-induced absorption bands that could not be detected from powder or solution spectra. Polarized absorption spectra on other compounds are necessary to elucidate these new features.

(18) Ferré, J.; Régis, M. *Solid State Commun.* **1978**, *26*, 225.

(19) Ferguson, J.; Guggenheim, H. J.; Krausz, E. R. *J. Phys. C: Solid State Phys.* **1971**, *4*, 1866.

(20) (a) Tanabe, Y.; Ebara, K. *J. Phys. Soc. Jpn.* **1971**, *30*, 886. (b) Day, P.; Dubicki, J. *J. Chem. Soc., Faraday Trans.* **1973**, *69*, 363. (c) Rodriguez, F.; Nunez, P.; Marco de Lucas, M. C. *J. Solid State Chem.* **1994**, *110*, 370.

Moreover, the interaction parameter was found to change sign between the ground state and the excited state. We hope to be able to rationalize this behavior soon.

Appendix

$$\Lambda = 2 \left[\frac{b_1}{3a_0} + \frac{b_0}{a_0} \right]$$

$$a_0 = 4 \left[\frac{\text{sh } v}{v} - \frac{\text{ch } v}{v^2} + \frac{1}{v^2} \right]$$

$$a_1 = 12 \left[\left(\frac{1}{v} + \frac{12}{v^3} \right) \text{sh } v - \left(\frac{5}{v^2} + \frac{12}{v^4} \right) \text{ch } v - \frac{1}{v^2} + \frac{12}{v^4} \right]$$

$$b_0 = \frac{1}{v} [\text{ch } v - 1]$$

$$b_1 = 3 \left[\left(\frac{1}{v} + \frac{4}{v^3} \right) \text{ch } v - \frac{4}{v^2} \text{sh } v + \frac{1}{v} - \frac{4}{v^3} \right]$$

with

$$v = - \frac{J[S_{\text{Mn}}(S_{\text{Mn}} + 1)]^{1/2}}{kT}$$

$$S_{\text{Mn}} = 5/2, \quad s_{\text{Cu}} = 1/2$$

where k is the Boltzmann constant.

Supporting Information Available: Listing of the calculation details of the intensity $I_i(T)$. This material is available free of charge via the Internet at <http://pub.acs.org>.

IC991264T